Journal of Advanced Joining Processes 1 (2020) 100024

Contents lists available at ScienceDirect

Journal of Advanced Joining Processes

journal homepage: www.elsevier.com/locate/jajp

Investigating plasma keyhole welding with multiple wires for fusion welding with chemically graded weld seams

F. Akyel*, L. Oster, S. Olschok, R. Sharma, U. Reisgen

RWTH Aachen University, Welding and Joining Institute, Aachen, Pontstr. 49, D-52062

ARTICLE INFO

Keywords:
Low Transformation Temperature (LTT)
multi-wire plasma keyhole welding
graded welding structure
mechanical properties
martensite start temperature (M_s)

ABSTRACT

Fusion welding processes are characterised by high temperature gradients, caused by the local heat input, which in turn leads to the formation of thermal and transformation induced (tensile-) stress. If the resulting stress exceeds the yield point, distortion occurs, which has a strong influence on the geometrical precision of the component. To counter these effects, in the past few years Low Transformation Temperature (LTT) materials were successfully used as filler wire. Here, the martensite start temperature is reduced and the increased thermal expansion during the martensitic phase transformation is used to induce compressive stress. Thus the formation of tensile stress through thermal shrinkage can be actively counteracted by the formation of compressive stress at reduced temperature. This counteracts the thermal distortion with the use of phase transformation. However, a solid technical solution for locally inducing LTT injections needs to be found. The following article presents a new approach of generating chemically graded weld seams in order to change the microstructure from ferritic to martensitic LTT alloy within the welding process. Therefore, a multi-wire plasma keyhole process is used to create a new alloy in-situ with varying nickel and chromium contents. To obtain a chemically graded structure the wire feed speeds are changed continuously within the welding process. For the multi-wire plasma keyhole process, a conventional plasma welding torch is extended by additional wire feeders, developed by the RWTH Aachen University Welding and Joining Institute. The graded structure is achieved by combining a high chromium-nickel filler wire with a conventional low alloy filler wire. The length of the graded area is varied so that the transition from high to low alloy area is either long or short. The results show, that it is possible to establish a stable welding process and change the chemical composition within the weld seam in-situ. Cross sections show a changing microstructure from low alloy ferritic microstructure to a martensitic microstructure. The influence of the transition area on the resulting microstructure and mechanical properties, such as hardness, is investigated. The experiments were performed in order to develop a basic knowledge about the mixing of dissimilar materials in plasma keyhole welding and the effects on the microstructure.

Introduction

Due to the constantly growing demands on steel constructions with regard to their geometrical precisions and strength, high-performance materials are used more frequently. However, welded constructions, made of high strength materials are of limited use, since the welded joints are susceptible to component distortion and even cracking due to constant use Kromm, 2011. This is due to the fact that the heat generated during welding causes a structural change in the welded joint. The local application of heat during the welding process generates various stress conditions in the component. The thermal processing results in a high temperature gradient between the weld seam and the base material. This results in an inhomogeneous stress distribution in the whole specimen and ultimately leads to residual welding stress. If the residual stresses exceed the yield point, plastic deformation occurs, which leads to distortion of the component. In order to avoid residual stresses, subsequent after-treatments must be carried out, such as stress-relief annealing or mechanical treatments like hammer-peening Reisgen et al., 2016; Dilthey et al., 2005; Radaj, 2012; David et al., 2003; Ueda et al., 1976 and Simoneau et al., 2009. In order to avoid distortion, most components are clamped restrictively in the welding process or straightened afterwards, which in turn leads to high residual tensile stresses within the welded specimen. A reduced tensile stress is desired since these structures show better properties such as fatigue life or sensitivity to hot and cold cracks, Azizpour et al., 2019. In order to counteract high-priced after-treatment, so-called Low Transformation Temperature (LTT) materials can be used. These materials are usually added to the process as filler materials and reduce distortion and, ideally, residual stress during cooling of the component. Here, the effect is exploited that the austenite to martensite phase transformation is being followed by a volumetric expansion and compressive stresses are induced in the weld seam, which counteract the high welding tensile stresses. Thus the com-

* Corresponding author.
E-mail address: akyel@isf.rwth-aachen.de (F. Akyel).

https://doi.org/10.1016/j.jajp.2020.100024
Received 12 November 2019; Received in revised form 9 April 2020; Accepted 9 April 2020

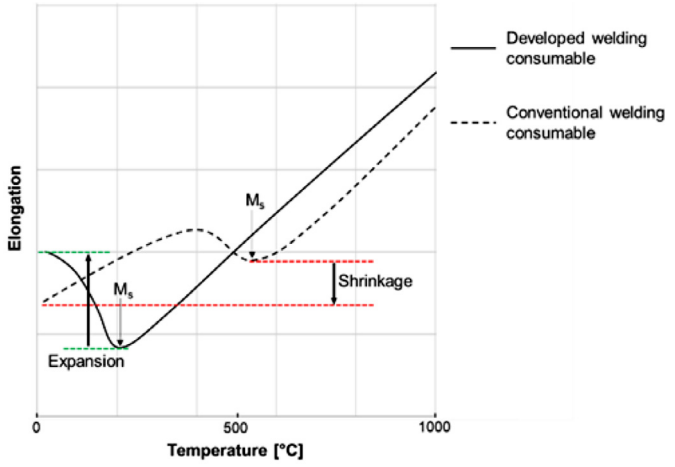

Fig. 1. Development of elongation depending on martensite start temperature (M_s) (Ohta et al., 1999).

ponent precision can be increased by in-situ alloying, Azizpour et al., 2019.

State of the Art

In the past few years the controlling of welding residual stress and distortion by means of phase transformation has been desired. In welded joints of steels, shrinkage and transformation residual stresses occur in the immediate weld seam area due to inhomogeneous temperature distribution and (in the case of transformable steels) phase transformation. To control residual stress and distortion, compressive stress in the weld seam by using the phase transformation during the cooling process is aimed. With this not only the residual stress within the weld seam is reduced but the mechanical behaviour of welded structures are also increased Masubuchi et al., 1993. The residual stress distribution is influenced to a significant extent by the phase transformation in addition to the restricted shrinkage Heeschen et al., 1988. This means residual stress in welded specimen is a superposition of phase transformations and thermal shrinkage Schulze et al., 2010. Thermal distortion cannot be influenced without further ado, however, the influence of phase transformation can be influenced by means of targeted alloying in order to build up further compressive stresses in the welded specimen.

For the transformation of martensite, two temperatures are of relevance: martensite start temperature (M_s), where the martensite formation begins, and martensite finish temperature (M_f), where the martensite is formed 100 % Martinez et al., 2005. When using conventional filler wire, cooling induced contraction occurs up to the point of phase transformation around 500°C. After the transformation, however, the contraction continues until a shrinkage can be recorded due to tensile residual stresses within the weld seam, Fig. 1. If the austenite to martensite transformation takes place at low temperatures (for example 200°C), this is referred to as the low-transformation-temperature (LTT) effect. Here the higher expansion by the martensite formation is used, which continues until the room temperature is reached. This leads ultimately to reduction of tensile residual stresses and distortion Bhadeshia 2002. If, however, M_s is reduced too much, martensite formation will not be completed since M_f drops below room temperature and shrinkage will occur again. As a result, retained austenite is formed in the heat affected zone. Therefore it is to take into account, that M_s must not be reduced too much Ohta et al., 1999.

There is no previous definition for the low transformation temperature material. In literature it is stated, that an LTT alloy is a filler material that uses a martensitic phase transformation temperature above room temperature and that the main difference to conventional filler material is the higher content of Cr and Ni (at least up to 10 m%). Kromm, 2011; Çam et al., 2010.

In the literature some investigations were carried out to calculate the martensite start temperature via the composition of the alloying elements, Payson et al., 1944; Carapella, 1944; Rowland et al., 1946; Grange et al., 1946; Steven et al., 1956 and Andrews et al., 1965. In Kung et al., 1982 some formulae were investigated regarding their accuracy in predicting the M_s temperature for high and low alloy steels. Research showed that the formulae of Steven and Haynes Steven et al., 1956 and Andrews Andrews et al., 1965 were the most accurate. Whereby the formula according to Steven and Haynes proved to be the most robust for high Cr contents. Since a high alloy filler wire with a high Cr content was used in this work, the Steven and Haynes formula is used, equation 1.

$$Ms = 561 - 474 \times C - 33 \times Mn - 17 \times Cr - 17 \times Ni - 21 \times Mo \quad (1)$$

In this study the homogeneous intermixing of two different filler wires was investigated in order to gain knowledge about the microstructure that will be formed and if an LTT effect could be used for further investigations. With the combination of a high alloy and a low alloy material a de-alloying of the high alloy material was aimed to gain a chemical composition that resembled the content of an LTT. Thus, the potential of in-situ alloying was investigated to produce the desired alloy composition during the welding process by using conventional filler wires. Since there is no real definition of how high the alloying elements in an LTT should look like, the effect of different alloying compositions was investigated by using a graded structure.

Welding Trials

Material. Two low alloyed sheets (S235JR) with the dimensions of 200 × 100 × 5 mm were butt welded lengthwise with the multi-wire plasma keyhole process in a single pass. Two filler wires were used in a graded structure (bead on plate with free root formation). A high alloy filler wire G 25 20 (EN ISO 14343-A G 25 20) and a low alloy filler wire G 3Si1 (EN ISO 16834-A G 3Si1) both by the company ESAB, Sweden, and both with 1 mm diameter were used during the welding trials. Argon (DIN EN ISO 14175: I1) was used as shielding gas, while H5 (DIN EN ISO 14175: R1-ArH-5) was used as plasma gas.

The chemical composition of the materials was measured using an Optical Emission Spectrometer (OES), **Table** 1. To be able to measure the thin filler wires, they were melted under inert gas atmosphere in ceramic crucibles into larger samples.

Experimental Setup. For the multi-wire plasma keyhole process, a conventional plasma welding torch was used, which was extended by an additional wire feed unit for 2 wires, Fig. 2. The wire feed speeds were controlled independently of each other by using a control computer, equipped with an analog out voltage module in combination with LabVIEW.

In order to obtain a chemically graded structure, the transition time between the two wires was changed, resulting in an area that has either a long or short graded pass, Fig. 3. The transition time of the short transition zone (STZ) was 3 s, whereas the transition time of the long transition zone (LTZ) was 26 s. This resulted in a STZ of 17.5 mm length, whereas the LTZ had a length of 145 mm.

Welding started with the high alloy filler wire (filler wire 1). After a defined welding time, the low alloy filler wire (filler wire 2) was added to the process, so that both filler wires were supplied simultaneously. While the wire feeding speed of filler wire 1 was gradually reduced, the feeding speed of filler wire 2 was increased in the same proportion, until the process was completed with filler wire 2 being fed only. Thus at the beginning of the weld a microstructure of dissimilar material com-

Table 1
Main alloying elements of the two filler wires and the base material (in m%).

Material	Fe	C	Si	Mn	Cr	Ni	Mo	P	S
S235JR	98.2	0.08	0.056	1.01	0.413	0.041	0.014	0.0338	0.0029
G 3Si1	97.4	0.09	0.09	1.35	0.02	0.02	<0.005	0.01	0.02
G 25 20	51.7	0.11	0.55	1.32	24.96	20.89	0.117	0.0187	0.0019

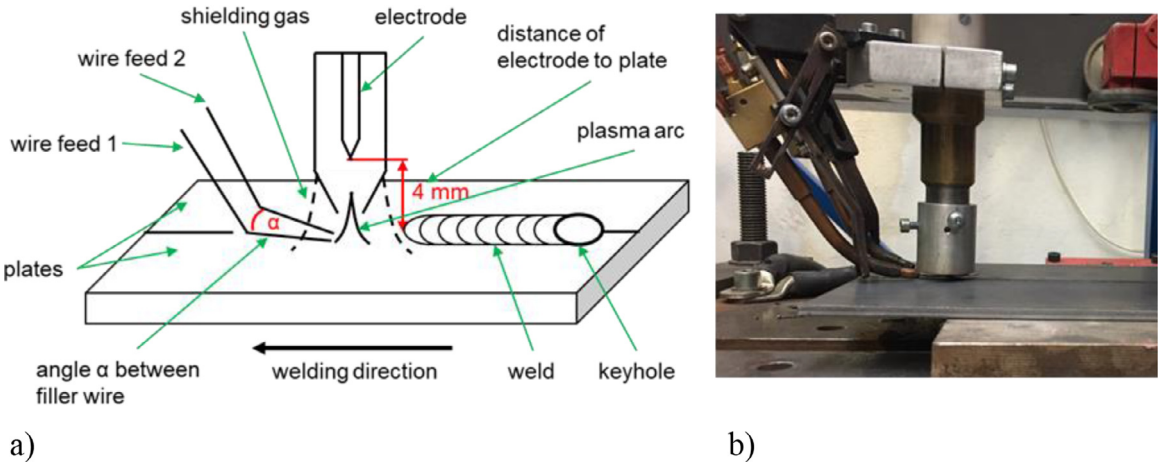

Fig. 2. Welding setup of plasma arc multi-wire process with two filler wires. a) Schematic picture of plasma multi wire welding, b) picture of the used plasma welding torch.

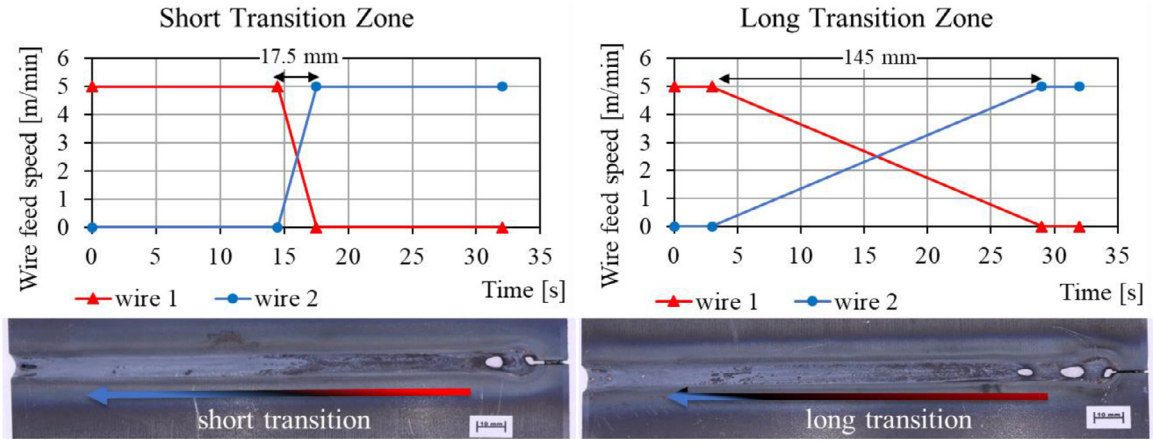

Fig. 3. Wire feed speed over time for short transition zone (STZ) and long transition zone (LTZ).

bination was produced and at the end of the weld a microstructure of similar material combination was produced. During the complete weldment, the summarized wire feed speed and therefore the deposition rate was kept constant. The influence of the chemical gradient and dissimilar welding on the mechanical properties (hardness) was investigated.

To investigate a suitable welding parameter set, pre experiments were performed. The goal was, to find a parameter window, which generates a stable keyhole and uniform weld seam geometry while the wire feed speeds were altered. As the viscosity of the high alloy filler wire was higher, compared to the low alloy wire, the arc intensity needed to be high enough to gain an equal weld seam shape. At the same time the heat input needed to be kept low enough, to keep the keyhole stable for the low alloy part of the weld seam. After investigating the optimum welding parameter, only the position of the transition zone varied throughout the process by changing the starting and ending time of the wire feeds, Table 2.

Results

Various tests were carried out to evaluate the welded samples. Metallographic examinations were carried out by transverse and longitudinal cross sections. Hardness measurements, macro and micro sections were made. For the investigation of the chemical composition line scans were carried out with an energy-dispersive X-ray spectroscope (EDS) investigation. The information on the chemical composition was used to calculate the theoretical martensite start temperature according to the formula of Steven and Haynes.

Microstructure. First, the cross section of a weld seam with a high alloy filler wire was examined, Fig. 4. It can be seen that carbides are present. The microstructure consisted mainly of austenite, bainite and martensite in contrast to the ferritic-pearlitic base material. Because of the nickel content, the formation of pearlite was suppressed. Although a dissimilar weld was present, the weld seam appeared to have been

Table 2
Welding parameters.

wire feed speed v_D [m/min]	welding speed v_S [m/min]	welding time t [s]	plasma gas f_P [l/min]	shielding gas f_S [l/min]	current I [A]
5	0,35	32	5	18	275

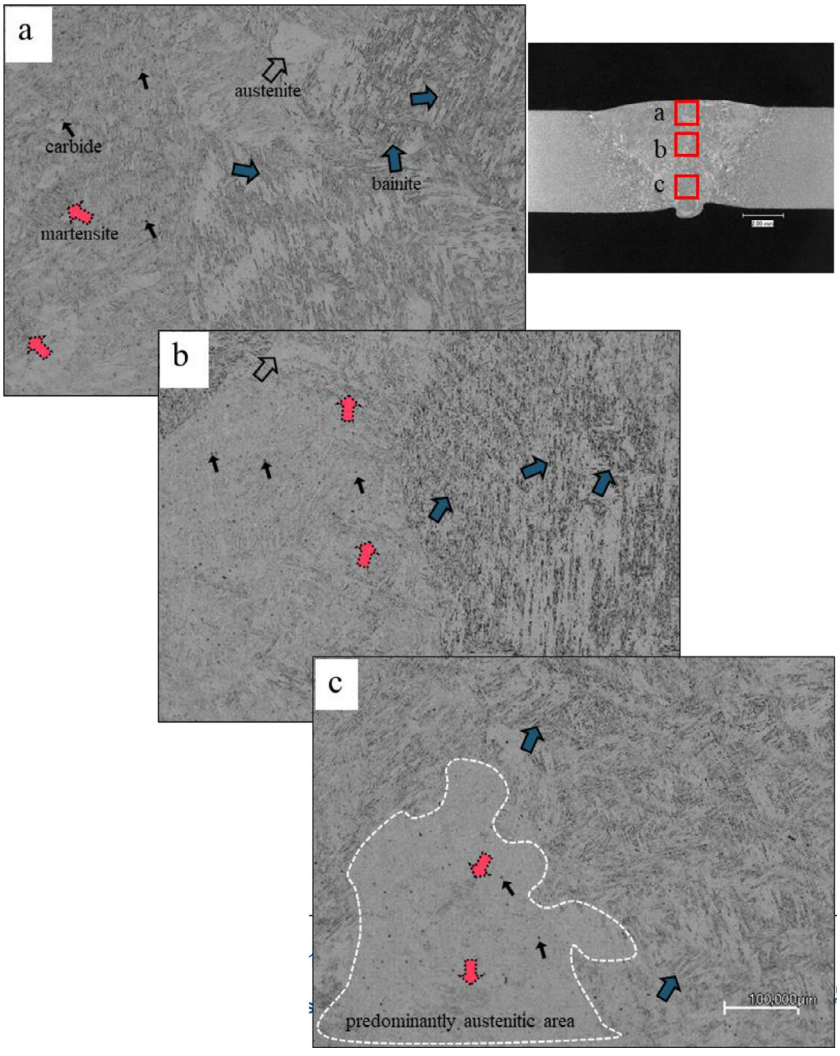

Fig. 4. Macro and micro cross sections of the welding zone with high alloy filler wire.

homogeneously mixed. Here, the micro images of the microstructure appeared comparable.

As the next step a cross section in the transition area was examined, Fig. 5. In the upper area of the weld a predominantly martensitic and bainitic microstructure could be observed. In the lower part of the weld, however, a mainly austenitic structure could be seen. Carbides were detected over the entire cross section. In the transition area, therefore, homogeneous intermixing of the two wires did not seem to occur.

Furthermore, the cross section with low alloy filler wire, i.e. a similar welding, was examined. A ferritic-pearlitic microstructure was determined, Fig. 6. Carbides were not present or were present in very small quantities. The structure of the upper and lower weld seam was identical due to the similar welding process.

In order to be able to further investigate the intermixing of the two filler wires in the transition zone, longitudinal sections of the samples with a long transition zone were prepared and analysed.

When considering the longitudinal section in the LTZ, it became clear that the intermixing between the two wires was initially inhomogeneous. The upper and lower areas of the weld seam could be clearly distinguished with regard to their microstructure, Fig. 7-**a**. As the proportion of low-alloyed material increases, the two regions appear to be becoming increasingly intermixed, Fig. 7-**b/c**. This continues up to a certain point with an apparent mixing of the two areas, so that no clear distinction between the two areas is possible from a mere macroscopic point of view, Fig. 7-**d**.

Hardness. To compare the hardness of each sample, a hardness series was recorded across the middle of the sample. The hardness according to Vickers (HV 0.2) was compared. The hardness of the base material was approx. 150 HV 0.2. The area with purely high alloy filler wire (dissimilar material combination), the transition area and the area with purely low alloy filler wire (similar material combination) were compared.

In the area with high alloy filler wire, a hardness increase of up to 400 HV 0.2 occurred, Fig. 8. An increase took place first over the fine grain and coarse grain zone of the weld until the maximum plateau within the weld has been reached.

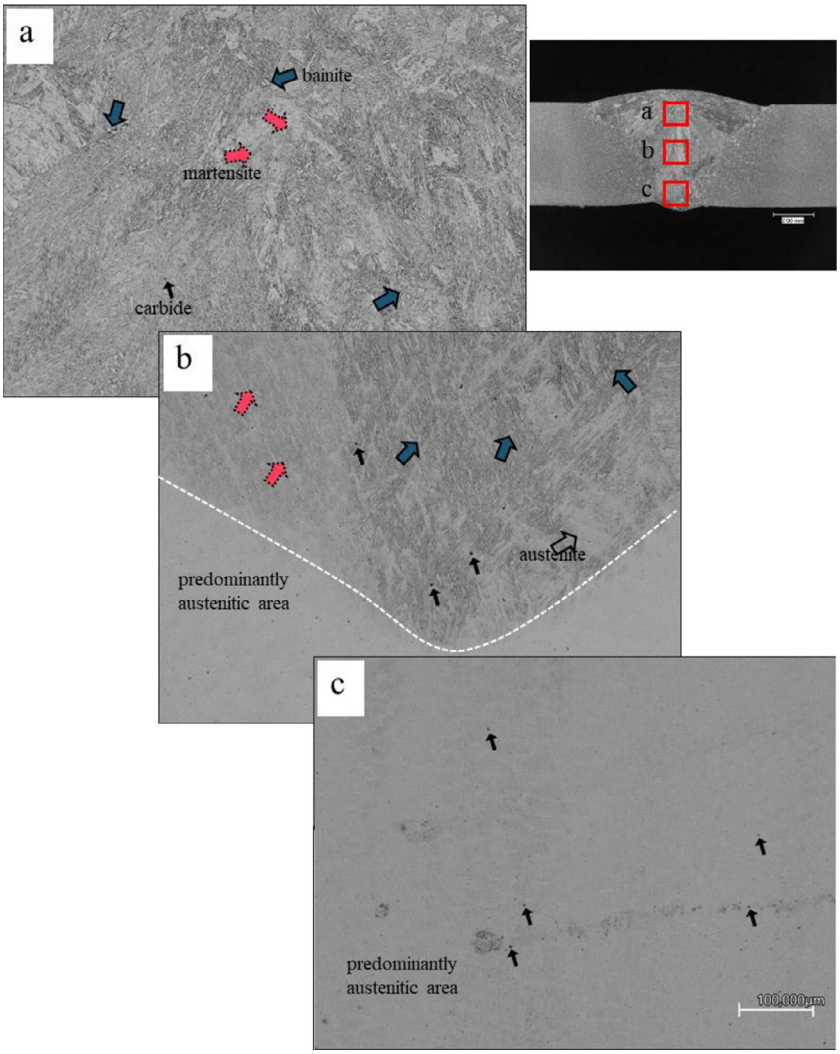

Fig. 5. Macro and micro cross sections of the transition zone.

The high hardness values in the weld seam showed that a structure with a higher hardness, such as martensite, was present in contrast to the ferritic-pearlitic base material microstructure.

This also applied to the transition zone, in which average hardness values of up to 380 HV 0.2 were achieved, Fig. 9. The longitudinal macro sections showed a difference in the upper and lower microstructure in the transition zone up to a certain length. This explains why the hardness values of the high alloy area and the transition zone are approximately the same. It can also be observed that the base material hardness of 150 HV 0.2 is reached at a greater distance from the weld seam center (around 6 mm) than the weld areas with purely high alloy filler wire (around 4.8 mm).

While hardening up to approximately 400 HV 0.2 occurred in the high alloy zone and in the transition area, the average hardness in the low alloy zone remained at approximately 230 HV 0.2, Fig. 10. With the similar welding no martensite was formed in the weld seam and thus the hardness was not increased that much.

From the samples with long graded area and short graded area 8 cross sections were taken at a distance of 15 mm each, starting from the area with high alloy filler wire (HA-1) over the transition zone (TZ-1) to the area with low alloy filler wire (LA-1). The weld start and ending was excluded up to 50 mm. For each cross section, the average of the hardness plateaus from the centre of the weld seam was recorded. Thus, the hardness curve could be documented over the entire sample length (with the exception of the weld start and weld end), Fig. 11.

A significant decrease in hardness could be determined for the hardness curve of the short-graded sample. The hardness dropped from 400 HV 0.2 to about 200 HV 0.2.

The hardness curve of the long graded specimen showed a slight decrease in hardness. The hardness value dropped from about 400 HV 0.2 to about 360 HV 0.2. Since the areas of the purely high alloy filler wire or purely low alloy filler wire were in the weld start or weld end, these were not covered in the cross sections. Nevertheless, it can be stated that even if the low alloy content increases, the hardness almost does not change. Even with a decreasing proportion of high-alloy wire in the weld metal, the amount is still sufficient to increase the hardness within the weld seam.

Energy-dispersive X-ray spectroscopy. In order to determine the chemical composition within the weld seam, the cross sections were examined using an EDS to perform line scans. As in the hardness measurements, the line scan measurement series was taken across the middle of the sample. In particular, the alloying elements used to calculate the M_s temperature (such as Mn, Cr, Ni and Mo) were examined more closely.

First, a line scan was carried out through a cross section in the high alloy area. The Cr content in the base material was in average about 0.38 m%, while the Ni content was about 0.07 m%. Within the weld seam, the Cr content increased in average to about 8.18 m%, while the

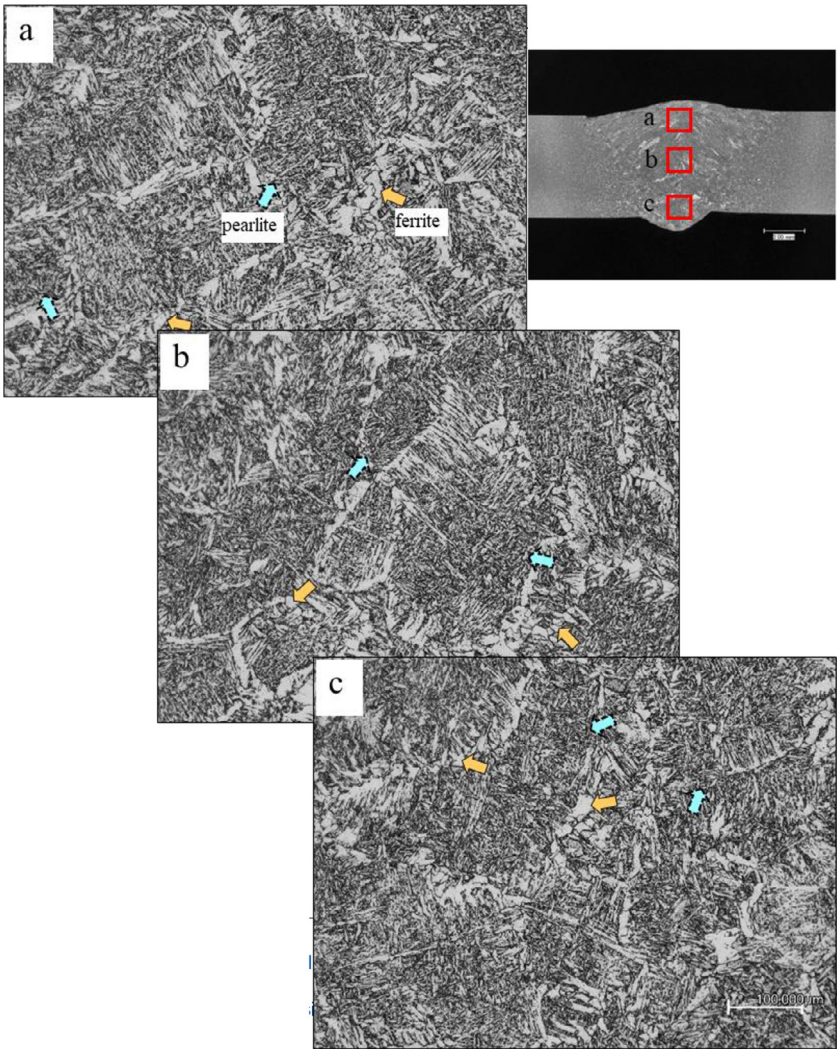

Fig. 6. Macro and micro cross sections of the welding zone with low alloy filler wire.

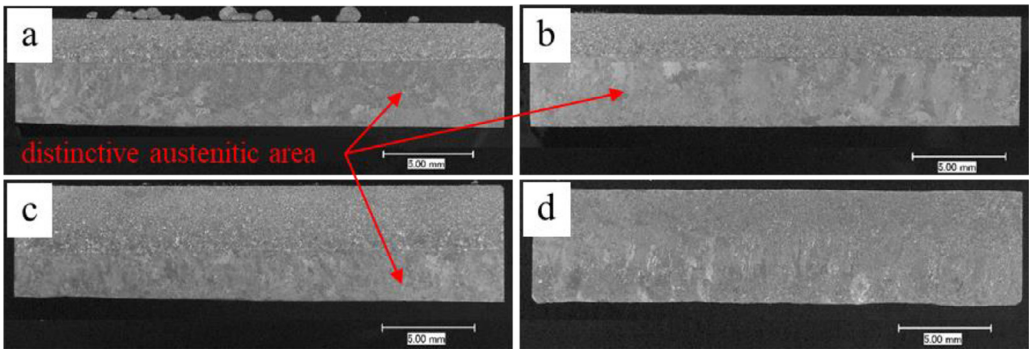

Fig. 7. Longitudinal sections of LTZ with distinctive austenitic area in the lower part of the weld.

Ni content increased to about 5.79 m%, Fig. 12. In contrast, the alloying elements Mn and Mo were not influenced by the high alloy filler wire noticeably, since the content of those two elements are nearly the same in the base material and the filler wire. This showed overall that the high alloy filler material caused an addition of Cr and Ni within the weld seam, whereas Mn and Mo was not influenced by it significantly.

In the transition zone, an increased Cr and Ni content could also be determined in contrast to the base material, Fig. 13. Overall, however, their proportions were somewhat lower than in the high alloy zone; while the Cr content was determined in average to about 4.27 m%, the Ni content was about 2.83 m%. This showed that the supply of the low alloy filler wire lead to the further de-alloying of the high alloy filler wire in that area, especially of the Cr and Ni elements.

The cross sections and longitudinal sections of the transition zone showed that the upper and lower areas of the weld seam had a different microstructure. This was investigated more closely in an EDS mapping in the middle left side of the weld seam and by EDS measurements in the upper (measure area 1) and lower (measure area 2) area of the weld seam, Fig. **14**.

The mapping showed once again the increase of the Cr and Ni content in the weld seam in contrast to the base material, whereby the Mn and Mo contents were not or only slightly changed. However, it was also

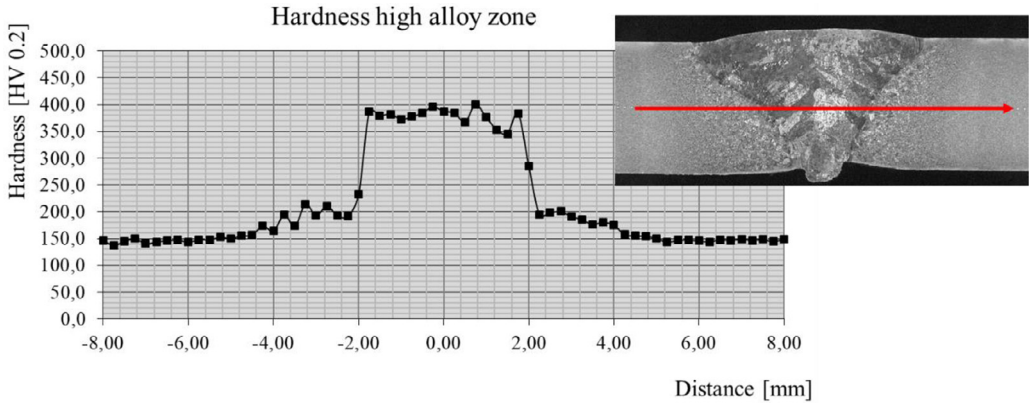

Fig. 8. Hardness propagation in the weld with high alloy filler wire.

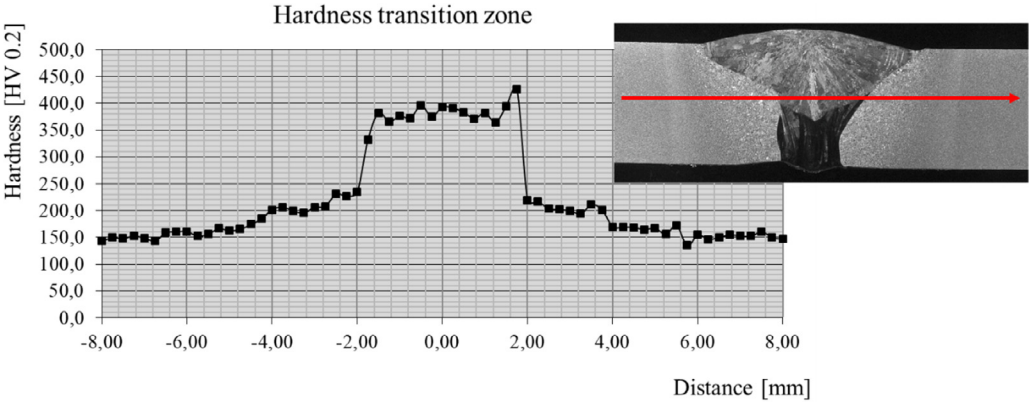

Fig. 9. Hardness propagation within the transition zone.

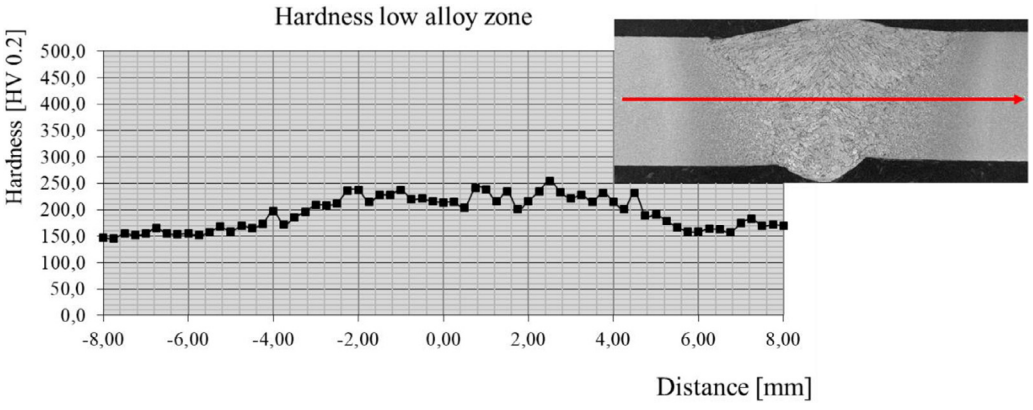

Fig. 10. Hardness propagation in the weld with low alloy filler wire.

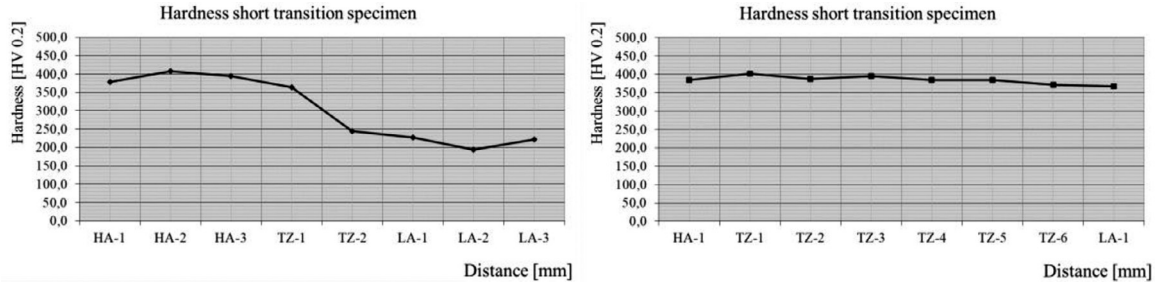

Fig. 11. Hardness propagation in average over the entire sample length.

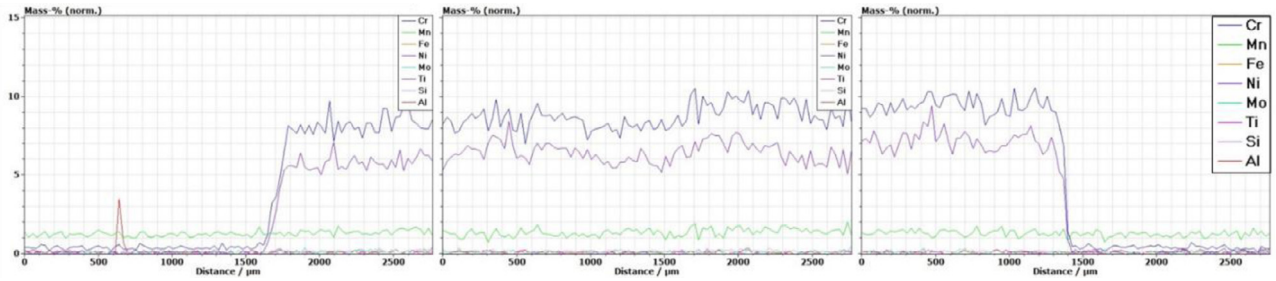

Fig. 12. EDS line scan across the middle of a cross section of the sample with high alloy filler wire.

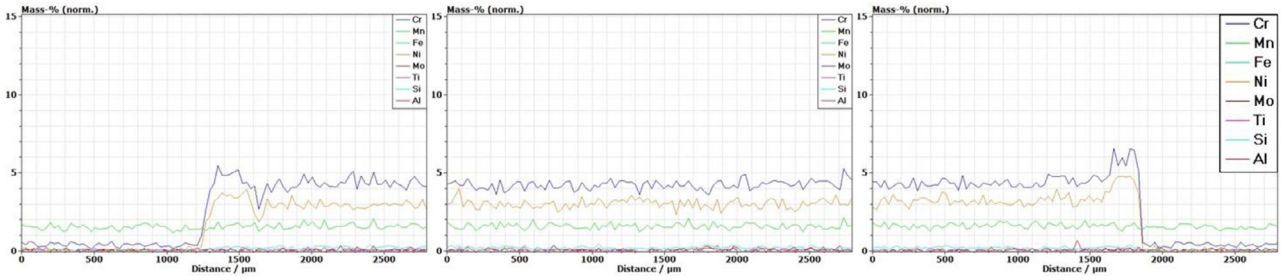

Fig. 13. EDS line scan across the middle of a cross section of the transition zone.

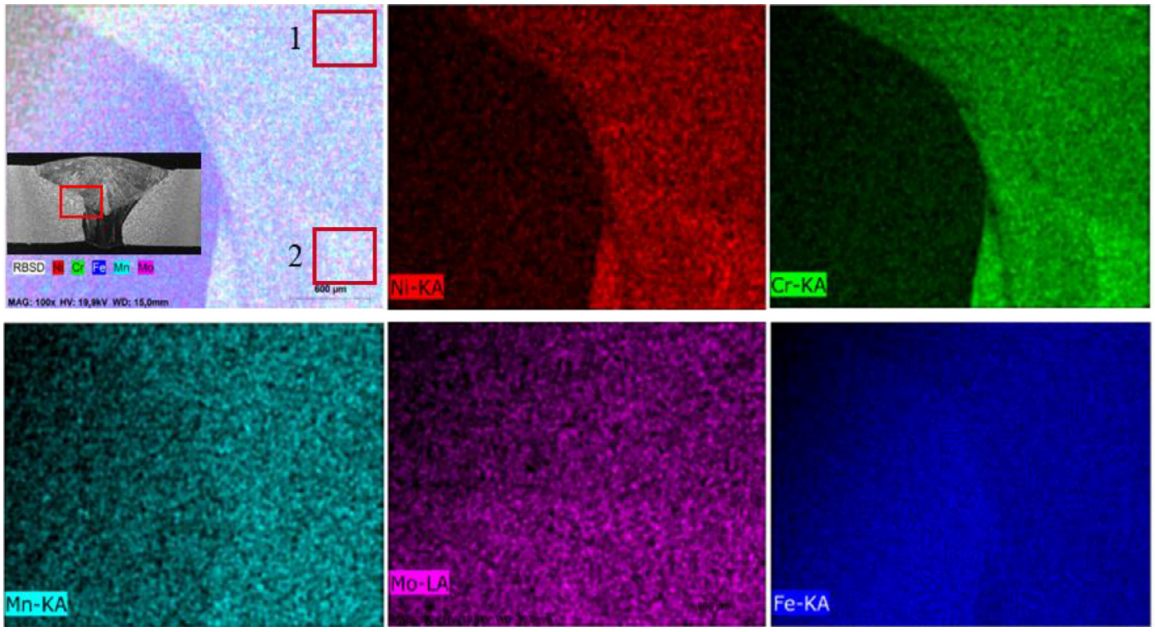

Fig. 14. EDS mapping of a cross section in the transition zone showing the higher Cr and Ni compared to the base material.

found that a higher Cr and Ni content could be measured in the lower part of the weld seam than in the upper part. An EDS measurement of measuring area 1 showed a Cr contend of around 3.93 m% and a Ni content of around 2.92 m%. This values increased in the measuring area 2 to 6.16 m% for Cr and 4.72 m% for Ni. The higher Ni content could explain why a more austenitic structure was found in the lower part of the weld seam, since Ni is austenite-stabilizing.

Further EDS line scan investigations were also carried out in the low alloy zone, with no major differences in the chemical composition of the weld in comparison to the base material due to the fact that the weld was of the similar type.

Martensite start temperature M_s. The martensite start temperature was calculated using equation 1. The chemical composition was taken from the line scan measurements and OES analysis. Since the carbon content cannot be measured reliably in the EDS measurement, upper and lower M_s values were calculated, whereby the C content of the base material (0.08 m% C) or the high alloy filler wire (0.11 m%) was used as maximum or minimum values. For the base material this resulted in a M_s temperature of about 474.4°C. Considering the high alloy zone, the martensite start temperature decreased in the weld seam because of the higher Cr and Ni contend, resulting in $M_{s,upper}$ of 238.9°C or a $M_{s,lower}$ of 224.7°C. Within the transition zone the martensite start temperature did not decrease that much, with an $M_{s,upper}$ of around 354.4°C or a $M_{s,lower}$ of 340.2°C. The M_s temperature did not change for the low alloy zone and was not calculated.

Conclusions

In contrast to the ferritic-perlitic base material, a microstructure consisting of martensite and bainite was found in the high alloy zone dur-

ing examination of the macro and micro sections. However, carbides were also found which can most probably be traced back to the high chromium content. In order to minimize the carbide content, either the Cr content or the C content would have to be reduced. Since both elements contribute strongly to the reduction of the M_s temperature and C is rather undesirable in welds, attempts should be made to keep it as low as possible for further experiments.

An inhomogeneous microstructure with carbides was found in the transition zone. While the upper part of the weld had a martensitic structure, the lower part appeared austenitic. In longitudinal sections the two zones could be separated macroscopically, whereby this separation disappeared with increasing proportion of low alloy filler wire. The mixing ratio from which this separation no longer takes place remains to be clarified. It is also quite conceivable that phenomena such as bath mixing or different densities of the molten high alloy or low alloy wire led to separation in the upper and lower areas of the melt bath. Since the high-alloy material has a higher density than the low-alloy material, this could explain why the austenitic material accumulates in the lower part of the weld. Further investigations will follow.

In the low alloy zone, a ferritic-perlitic microstructure as in the base material was found. No carbides were present here, which further confirms the assumption that the carbides present in the high alloy zone or the transition zone are chromium carbides.

When looking at the hardness measurements, an increase of the hardness up to about 400 HV0.2 was found in the high alloy zone as well as in the transition area, which was due to the presence of harder microstructures such as martensite. In the low alloy zone, however, the increase in hardness was less in comparison.

Overall, the measured hardness plateaus were examined on average. It was found that there was a slight decrease in hardness over a larger range in the samples with a long transition zone. This shows that even with the gradual reduction of the high-alloy content in the long-graded area, the chemical elements are still present in sufficient quantities to cause hardening of the structure. In the samples of the short transition zone, a higher decrease in hardness over a shorter range was present. Since the zones of the purely high-alloy filler wire and the purely low-alloy filler wire are relatively long, the decrease in hardness can be seen quite clearly over the short transition zone. How this affects the mechanical-technological properties has to be investigated further.

After considering the longitudinal sections, it was proven that welding and mixing of two wires was possible to a certain extent without pore formation or defects in the weld seam. The mixing ratio at which the separation of the zones no longer occurs still has to be clarified, but it was clearly visible that the samples with long transition zone showed separation over a long range. Nevertheless, it can be stated that a martensitic microstructure can be produced locally by using a high alloy filler wire.

On the basis of the EDS measurements the chemical composition of the welded specimen could be investigated. The addition of the high alloy filler wire led to an increase in the Ni and Cr contents in the weld seam, whereby the Mn and Mo contents were not significantly influenced. The investigations of the chemical compositions in the upper and lower part of the weld seam in the transition zone revealed that the Cr and Ni contents in the lower part was higher. Since Ni is an austenite former, this is considered to be the explanation for the austenitic structure in the lower part of the weld seam.

After calculations of the martensite start temperature, it could be shown that in the high alloy zone, the M_s could be reduced to about 220°C. Whether this is sufficient to reduce the residual stresses or minimize the distortion must be further investigated. The main goal was to create an LTT microstructure by in-situ alloying using conventional methods. It could thus be shown that the generation of an LTT structure was possible by using multi-wire plasma keyhole process.

Acknowledgments

The presented investigations were carried out at RWTH Aachen University Welding and Joining Institute ISF within the framework of the Collaborative Research Centre SFB1120-236616214 “Bauteilpräzision durch Beherrschung von Schmelze und Erstarrung in Produktionsprozessen” and funded by the Deutsche Forschungsgemeinschaft e.V. (DFG, German Research Foundation). The sponsorship and support is gratefully acknowledged.

Special thanks also go to the companies ESAB AB and EWM AG for providing welding consumables and welding machines.

References

Andrews, K.W., 1965. Empirical formulae for calculation of some transformation temperatures. J. Iron Steel Inst. 203, 721.

Azizpour, K., Moshayedi, H., Sattari-far, I., 2019. Application of low transformation-temperature filler to reduce the residual stress in welded component. J. Mech. Eng. Sci. 13, 4536.

Bhadeshia, H., 2002. Martensite in steels. Mat. Sci. Metall..

Çam, G., Özdemir, O., Koçak, M., 2010. Progress in low transformation temperature (LTT) filler wires (Proceedings of the 63rd Annual Assembly & International Conference of the International Institute of Welding. Istanbul.

Carapella, L.A., 1944. Computing A or MS (transformation temperature on quenching) from analysis. Met. Prog. 46, 108.

David, S.A., Babu, S.S., Vitek, J.M., 2003. Welding: Solidification and Microstructure. JOM 55, 14–20.

Dilthey, U., 2005. Schweißtechnische Fertigungsverfahren 2 – Verhalten der Werkstoffe beim Schweißen. Springer Verlag, Berlin Heidelberg, pp. 59–81.

Grange, R.A., Stewart, H.M., 1946. The temperature range of martensite formation. Trans. AIME 167, 467.

Heeschen, J., Nitschke, Th., Theiner, W.A., Wohlfahrt, D.H., 1988. Schweißeignung – Grundlagen, Bedeutung und Auswirkung in geschweißten Bauwerken. DVS Berichte 112, 109.

Kromm, A., 2011. Umwandlungsverhalten und Eigenspannungen beim Schweißen neuartiger LTT-Zusatzwerkstoffe Ph.D. thesis. BAM Dissertationsreihe Band 72.

Kung, C.Y., Rayment, J.J., 1982. An Examination of the Validity of Existing Empirical Formulae for the Calculation of Ms Temperature. Metallurgical Transactions A 13A, 328.

Martinez, F., Liu, S., 2005. Development of compressive stress in structural steel weld toes by means of weld metal phase transformations (Proceedings of the 7th International Conference Trends in Welding Research, Pine Mountain.

Masubuchi M., Recent MIT research in residual stresses and distortion on welded structures (1993)

Ohta, A., Watanabe, O., Matsuoka, K., et al., 1999. Fatigue strength improvement by using newly developed low transformation temperature welding material. WELD WORLD 43, 38.

Payson, P., Savage, C.H., 1944. Martensite Reactions in Alloy Steels. Transactions ASM 33, 261.

Radaj, D., 2012. Heat Effects of Welding: Temperature Field, Residual Stress, Distortion. Springer Science & Business Media.

Reisgen, U., Olschok, S., Gach, S., 2016. Nutzung von Low-Transformation-Temperature-Werkstoffen (LTT) zur Eigenspannungsreduzierung im Elektronenstrahlschweißprozess. Mat.-wiss. u. Werkstofftech.

Rowland, E.S., Lyle, S.R., 1946. The application of MS points case depth measurement. Trans. ASM 37, 27.

Schulze, A., 2010. Die Metallurgie des Schweissens Eisenwerkstoffe – Nichteisenmetallische Werkstoffe. Springer-Verlag.

Simoneau, R., Thibault, D., Fihey, J.-L., 2009. A Comparison of Residual Stress In Hammer-Peened, Multi-Pass Steel Welds – A514 (S690Q) and S41500. WELD WORLD 53, 124–134.

Steven, W., Haynes, A.G., 1956. The temperature formation of martensite and bainite in low–alloy steels, some effects of chemical composition. J. Iron Steel Inst. 183, 349.

Ueda, Y., Takahashi, E., Fukuda, E., et al., 1976. Multipass Welding Stresses in Very Thick Plates and Their Reduction from Stress Relief Annealing. Trans. JWRI 5:2, 179–189.